

Fundamental defect centers in glass: ^{29}Si hyperfine structure of the nonbridging oxygen hole center and the peroxy radical in $\alpha\text{-SiO}_2$

D. L. Griscom and E. J. Friebele

Naval Research Laboratory, Washington, D. C. 20375

(Received 7 August 1981)

^{29}Si hyperfine structure determinations for two fundamental oxygen-associated paramagnetic defect centers in high-purity amorphous silica complete the characterization of the nonbridging oxygen hole center and the peroxy radical by demonstrating in each case that the oxygen(s) trapping the unpaired spin are bonded to only one silicon in the glass network. It is shown that these findings place important constraints on the supposed precursors of the peroxy radical in $\alpha\text{-SiO}_2$.

Three distinct radiation-induced defect centers have been previously delineated in high-purity (≤ 1 ppm foreign cations) amorphous silica ($\alpha\text{-SiO}_2$). They are the E' center,¹⁻³ the nonbridging oxygen hole center (NBOHC),⁴ and the peroxy-radical hole trap.⁵ Atomic arrangements and wave-function densities at the defect sites have been deduced from ^{29}Si and ^{17}O hyperfine structure (hfs) observed in the electron-spin resonance (ESR) spectra of these defects. The most fully characterized in this regard has been the E' center. The structures of the NBOHC and peroxy radical defects have been inferred from their ^{17}O hfs alone, leaving open questions regarding their next-nearest-neighbor environments. Friebele *et al.*⁵ hypothesized that the peroxy radical is bonded to a single silicon in the glassy network, whereas Edwards and Fowler⁶ have lately calculated that for Si-Si distances typical of α quartz ($\sim 3 \text{ \AA}$), an intervening peroxy radical would be symmetrically bonded to both silicons. We report here a study of the ^{29}Si hfs of the NBOHC and the peroxy radical in $\alpha\text{-SiO}_2$.

Samples included silicas enriched to 99.98 at. % ^{28}Si ($I=0$) and 95.3 at. % ^{29}Si ($I=\frac{1}{2}$) obtained from Oak Ridge National Laboratory and 4-mm-diam rods of Suprasil 1 and Suprasil W1, a pair of high-purity fused silicas containing ~ 1200 and ≤ 5 ppm OH, respectively. The isotopically enriched samples were vitrified and dried in air at 1000°C for 93 h prior to ^{60}Co γ irradiation as described previously.² Data provided by Vitko⁷ indicated that similarly treated Suprasil 1 outgasses $\sim 70\%$ of the OH groups originally present. It was known from previous studies^{4,8} that both NBOHC's and peroxy radicals are formed in as-delivered high-purity fused silicas, with the NBOHC's predominating in the materials containing ~ 1200 ppm OH and the peroxy radical predominating in the products containing ~ 5 ppm OH. Post-irradiation heat treatments to 500°C were found to destroy all defect centers in Suprasil 1 while suppressing virtually *all centers but the peroxy radical* in

Suprasil W1.⁴ It was discovered in the present work that the partially outgassed isotopically enriched samples exhibited a spectrum dominated by the NBOHC immediately following γ irradiation (as does Suprasil 1), but that their post-irradiation annealing behaviors more nearly paralleled that of Suprasil W1.

Contamination of isotopically enriched silica samples by aluminum has been previously recognized⁴ as a potential problem in unraveling the radiation-induced ESR spectra of $\alpha\text{-SiO}_2$. In Fig. 1(b) four weak peaks indicated by arrows are identified as ^{27}Al ($I=\frac{5}{2}$) hfs of the $[\text{Al}]^0$ center⁹⁻¹¹ on the basis of a direct overlaying of the spectrum of an irradiated Al-

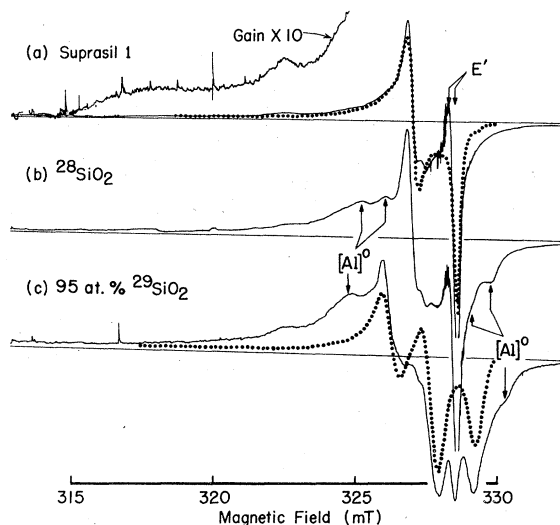


FIG. 1. X-band (9.2 GHz) ESR spectra obtained at 77 K for powdered samples of (a) Suprasil 1, (b) ^{28}Si -enriched silica, and (c) ^{29}Si -enriched silica following exposure to 3.2×10^8 -rad (Si) ^{60}Co γ rays at room temperature. Dotted curves are computer simulations of the NBOHC components referenced to sloping baselines.

doped silica sample (see, e.g., Ref. 11). These peaks are absent in the spectrum of high-purity Suprasil 1 [Fig. 1(a)]. If it is assumed that the ^{28}Si - and ^{29}Si -enriched samples are equally contaminated, then the peaks designated by arrows in Fig. 1(c) are logically ascribed to $[\text{Al}]^0$ defects which are interacting with both ^{27}Al and ^{29}Si nuclei. The $[\text{Al}]^0$ center has been characterized in the SiO_2 polymorph α quartz as a hole trapped on an oxygen bridging between a silicon and substitutional Al in the crystal framework.⁹ By comparing the field positions of the extremal peaks of the $[\text{Al}]^0$ spectra of Figs. 1(b) and 1(c), a ^{29}Si hfs splitting ~ 1 mT (10 G) can be deduced, lending incidental support to the common belief^{10,11} that the structure of the $[\text{Al}]^0$ defect in α - SiO_2 is similar to that in α quartz. Significant from the standpoint of the present study is the fact that the $[\text{Al}]^0$ spectrum in the isotopically enriched samples is sufficiently broad and weak that it does not seriously mask the principal spectra observed in the high-purity material [compare Fig. 1(b) with Fig. 1(a)]. Thus an analysis of the ^{29}Si hfs of the NBOHC is still feasible despite the aluminum contamination.

The dotted curve of Fig. 1(c) represents a best-fit computer simulation of the ^{29}Si hfs of the NBOHC assuming a hyperfine interaction with a single silicon and utilizing as a constraint the g -value distribution which resulted in the best fit^{4,8,12} of the Suprasil 1 spectrum of Fig. 1(a). The hfs splittings $A_1 = A_2 = 1.44$ mT employed in the simulation are identical with those determined⁸ for the HC_1 defect in alkali silicate glasses. On the basis of ^{29}Si and ^{17}O hfs, HC_1 has been attributed^{8,13} to a hole 100% localized in a pure $2p$ orbital of an oxygen bonded to a single silicon in the glass network. Due to the overlapping $[\text{Al}]^0$ and peroxy radical components, $A_1(^{29}\text{Si})$ and $A_2(^{29}\text{Si})$ for the NBOHC could be measured with an estimated precision of only $\sim \pm 0.1$ mT. In the case of HC_1 , there were no interfering components so the computer fits⁸ were sensitive to variations in A_1 or $A_2 \sim \pm 0.02$ mT. [$A_3(^{29}\text{Si})$ cannot be estimated for either the NBOHC or the peroxy radical in α - SiO_2 due to the obscuring effects of broad distributions in g_3 values (cf. Ref. 4)]. Subject only to the present reduced precision, it can be concluded that the structure of the NBOHC is essentially equivalent to that of HC_1 ; i.e., each defect comprises a hole trapped on an oxygen bonded to a single silicon in the glass network (nonbridging oxygens).

Figure 2 illustrates the peroxy-radical spectra observed in Suprasil W1 and three isotopically enriched silicas following γ irradiation and subsequent 10-min anneals at 500°C . Comparison of parts (a) and (b) of Fig. 2 shows that impurity effects are absent from the ^{28}Si -enriched sample and by implication also from the samples enriched in ^{29}Si . The spectrum of Fig. 2(a) was computer simulated as before^{4,12} (dotted curve) and the g -value distributions so determined

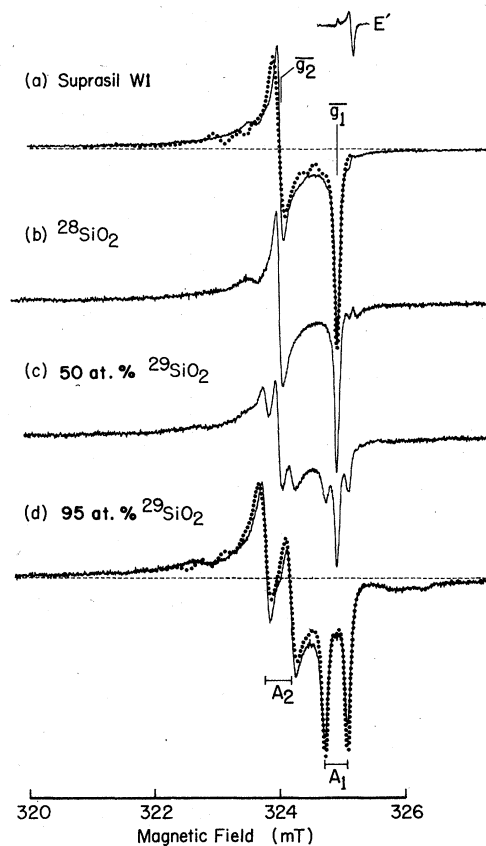


FIG. 2. X-band (9.1-GHz) ESR spectra obtained at 100 K for γ -irradiated fused silica samples following heat treatment at 500°C for 10 min: (a) 4-mm rod of Suprasil W1; (b) ^{28}Si -enriched silica; (c) a glass prepared from 50 at. % $^{28}\text{SiO}_2$ and 50 at. % $^{29}\text{SiO}_2$; (d) ^{29}Si -enriched silica. Irradiation doses were 5.9×10^7 rad for Suprasil W1 and 8.3×10^8 rads for the isotopically enriched samples. Dotted curves are computer simulations of the peroxy radical components, using Lorentzian convolution functions having p - p derivative widths of 0.035 and 0.046 mT for (a) and (d), respectively. The E' center resonance recorded 90° out of phase (inset) served as a g -value reference.

were used as constraints in the simulation of Fig. 2(d) (dotted curve). In this manner, the ^{29}Si hfs parameters of the peroxy radical were determined to be $A_1 = 0.36$ mT and $A_2 = 0.42$ mT with precisions $\sim \pm 0.01$ mT. These results demonstrate that (i) the resolved ^{29}Si hfs splittings of the peroxy radical arise from a single silicon, with any unresolved structure due to a second silicon being at least 5 times weaker (based on the convolution linewidth employed in the simulation), (ii) the magnitudes of the resolved splittings are $\sim 30\%$ of those which characterize the NBOHC, and (iii) $A_1(^{29}\text{Si})$ and $A_2(^{29}\text{Si})$ are not precisely equal, in contrast to the case for the NBOHC. The significance of conclusion (i) is that it supports the formation mechanism postulated by Friebele

*et al.*⁵ [Fig. 3(a)] and weighs against the mechanism of Edwards and Fowler⁶ [Fig. 3(b)], at least with regard to the peroxy radical population which survives the post-irradiation anneal at 500 °C. Result (ii) is consistent with the 25:75 distribution of spin density over the two peroxy oxygens deduced⁵ from the ¹⁷O hfs and supports the suggestion⁵ that the larger spin density resides on the oxygen more distant from the silicon to which the group is bonded. Finally, observation (iii) demonstrates¹⁴ that the O–O–Si bond angle must be less than 180°, as schematically drawn in Fig. 3(a).

The model of Fig. 3(a) implies the existence of bridging peroxy linkages in the unirradiated glass, presumably as members of Frenkel defect pairs comprising oxygen vacancies (Si–Si bonds which result in *E'* centers after irradiation) as the complementary members.⁵ Of course, additional defect pairs might be created by ionizing radiation sufficiently energetic to effect oxygen displacements. The preexistence of some peroxy linkages in low-OH silicas such as Suprasil W1 is indicated by the ability to form peroxy radicals by merely drawing the glasses into fibers and subjecting them (without irradiation) to subsequent annealing schedules in the range ~20–400 °C.^{4,15} Apparently, a sufficiently strained Si–O–O–Si linkage is vulnerable to thermal cleavage by shedding an electron as illustrated in Fig. 3(a). On the other hand, the calculations of Edwards and Fowler⁶ have shown that *unstrained* peroxy linkages are quite stable, i.e., in cases where the Si–Si distances are ~4–5 Å. Thus, the appearance of additional peroxy radicals observed⁴ upon annealing irradiated, low-OH silicas near 250 °C (with the destruction of an equivalent number of *E'* centers) could well arise from the O₂ diffusion mechanism proposed by Edwards⁶ [left-hand side of Fig. 3(b)] rather than

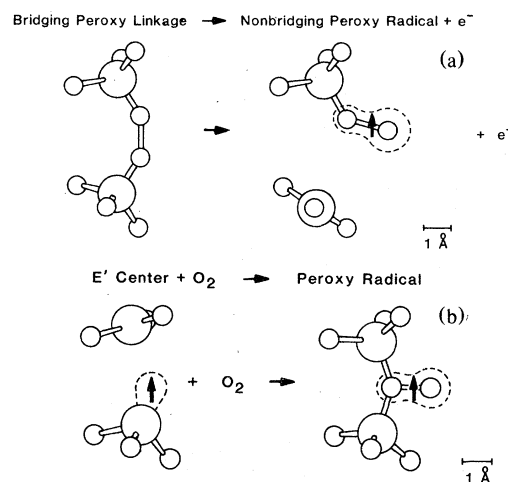


FIG. 3. Models for the formation of peroxy-radical defects in *a*-SiO₂ proposed in (a) Ref. 5 and (b) Ref. 6. In these schematic diagrams the unpaired spin occupies oxygen 2*p* orbitals perpendicular to the projection plane defined by the Si–O–O bonding.

electron shedding by peroxy linkages. The failure to observe the hypothetical defect represented on the right-hand side of Fig. 3(b) is explained if large relaxations were to take place at the *E'* sites such that the Si–Si separations exceed ~5 Å. Some evidence for this suggestion is the apparent absence of the expected “weak” ²⁹Si hfs due to the second silicon at the *E'* sites in *a*-SiO₂.³ Regardless of the actual formation mechanism, the present study has conclusively demonstrated the peroxy radical to have the structure illustrated on the right-hand side of Fig. 3(a).

A. Edwards and W. B. Fowler are gratefully thanked for advance communication of their results cited above.

¹R. A. Weeks, *J. Appl. Phys.* **27**, 1376 (1956); R. H. Silsbee, *ibid.* **32**, 1459 (1961); F. J. Feigl, W. B. Fowler, and K. L. Yip, *Solid State Commun.* **14**, 225 (1974).

²D. L. Griscom, *Phys. Rev. B* **20**, 1823 (1979).

³D. L. Griscom, *Phys. Rev. B* **22**, 4192 (1980).

⁴M. Stapelbroek, D. L. Griscom, E. J. Friebele, and G. H. Sigel, Jr., *J. Non-Cryst. Solids* **32**, 313 (1979).

⁵E. J. Friebele, D. L. Griscom, M. Stapelbroek, and R. A. Weeks, *Phys. Rev. Lett.* **42**, 1346 (1979).

⁶A. Edwards, Ph.D. thesis (Lehigh University, Bethlehem, Penn., 1981) (unpublished); A. Edwards and W. B. Fowler (unpublished).

⁷J. Vitko, Jr., and J. E. Shelby (unpublished).

⁸D. L. Griscom, *J. Non-Cryst. Solids* **31**, 241 (1978).

⁹For a review, see, J. A. Weil, *Radiat. Eff.* **26**, 261 (1975).

¹⁰R. Schnadt and A. Rüber, *Solid State Commun.* **9**, 159 (1971).

¹¹D. L. Griscom, in *The Physics of SiO₂ and Its Interfaces*, edited by S. T. Pantelides (Pergamon, New York, 1978), p. 232.

¹²The *g* values employed in the computer simulations of Figs. 1 and 2 were virtually identical with those derived in Ref. 4 except for an adjustment in the value of *g*₁ for the NBOHC from 2.0010 to 1.9999 and a shift of +0.0004 in the distributions of *g*₁ and *g*₂ which characterize the peroxy radical.

¹³D. L. Griscom, *J. Non-Cryst. Solids* **40**, 211 (1980).

¹⁴An analysis of the peroxy-radical *g* matrix [cf. W. Känzig and M. H. Cohen, *Phys. Rev. Lett.* **3**, 509 (1959)] shows that the axis of the large *g* shift *g*₃ is parallel to the O–O bond axis, while that of *g*₁(*A*₁) must be normal to the plane defined by O–O–Si and that of *g*₂(*A*₂) is by definition perpendicular to the axes of *g*₃ and *g*₁. Thus, in general, *A*₁ ≠ *A*₂ unless ∠(O–O–Si) = 180°. Conversely, for the NBOHC the axis of *g*₃ corresponds to the Si–O (nonbridging) direction and the observed situation *A*₁ = *A*₂ becomes expected (cf. Ref. 8).

¹⁵E. J. Friebele, G. H. Sigel, Jr., and D. L. Griscom, *Appl. Phys. Lett.* **28**, 516 (1976).